Theory of Electrostatic Probes in a Low-Density Plasma

Ira B. Bernstein and Irving N. Rabinowitz

Citation: The Physics of Fluids **2**, 112 (1959); doi: 10.1063/1.1705900
View online: http://dx.doi.org/10.1063/1.1705900
View Table of Contents: http://aip.scitation.org/toc/pfl/2/2
Published by the American Institute of Physics

Theory of Electrostatic Probes in a Low-Density Plasma

IRA B. BERNSTEIN AND IRVING N. RABINOWITZ
Project Matterhorn, Princeton University, Princeton, New Jersey
(Received November 12, 1958)

The theory of sperical and cylindrical probes immersed in plasmas of such low density that collisions can be neglected is formulated. The appropriate Boltzmann equation is solved, yielding the particle density and flux as functionals of the electrostatic potential, the situation in the body of the plasma, and the properties of the probe. This information when inserted in Poisson's equation serves to determine the potential, and hence the probe characteristic. No *a priori* separation into sheath and plasma regions is required. Though amenable to a determination of the full probe characteristic, the method is applied in detail and numerical results are presented only for the collection of monoenergetic ions, for the case of negligible electron current. These results indicate that the potential is not so insensitive to ion energy as has been believed, and that if the probe radius is sufficiently small, there enters the possibility of a class of ions which are trapped near the probe in troughs of the effective radial potential energy. The population of these trapped ions is determined by collisions, however infrequent. It is difficult to calculate, and conceivably can have a marked effect on the local potential.

INTRODUCTION

THIS work presents a method suitable for the computation of the characteristics of electrostatic probes in cases where collisions are negligible.[1] The method is applicable only to probes of such symmetry that the charged particle orbits can be characterized in terms of explicit time-independent constants of the motion. In particular the scheme has been applied to the collection of positive ions by spherical and cylindrical probes. The method is completely self-consistent, and requires no *a priori* separation of the discharge into plasma and sheath.

The method relies on the fact that in the absence of collisions the general solution of Boltzmann's equation for a particle distribution function is an arbitrary function of the constants of motion.[2] The precise function is determined completely by boundary conditions, namely the flux of incoming particles at some large radius past which collisions become important, and the absorptive and reflective properties of the probe. Knowledge of the distribution function permits computation of the particle density and flux, essentially as functionals of the electrostatic potential. Poisson's equation then serves to determine the potential.

Numerical computations are presented for the collection by completely absorbing probes of monoenergetic ions, assuming that the collection of electrons is negligible. These indicate (a) that the ion temperature is more significant in determining the probe characteristic than has been believed,[3] and (b) that if the probe radius is sufficiently small, there exists the possibility of orbits of bounded extent (trapped ions) whose populations are determined by collisions.

[1] Allen, Boyd, and Reynolds, Proc. Phys. Soc. (London) **B70**, 297 (1957). This paper contains a review of past theory of the collection of positive ions, and appropriate references.

[2] K. M. Watson, Phys. Rev. **102**, 12 (1956).

SPHERICAL PROBE

Consider a spherical probe of radius R immersed in a plasma composed of electrons, and one kind of positive ion. Denote radial distance from the center of the probe by r. Assume that the electrostatic potential $\phi(r)$ is negative at the probe and rises monotonically to zero as one moves radially outward into the body of plasma.* Let e be the magnitude of the charge of the electron, Ze the charge of the ion, T_e the electron temperature in the body of the discharge, T_i the ion temperature in the body of the discharge, N_0 the electron density in the body of the discharge, and λ the effective mean free path for ion collisions. Assume that

$$-e\phi(R) \gg KT_e, \qquad \lambda \gg R. \tag{1}$$

Then very few electrons can reach the probe and to a very high degree of approximation the electrons are in kinetic equilibrium. Thus there is no net electron current, and the electron density is given closely by

[3] D. Bohm, in *The Characteristics of Electrical Discharges in Magnetic Fields*, A. Guthrie and R. K. Wakerling, editors (McGraw-Hill Book Company, Inc., New York, 1949), Chap. 3.

* The general method can be applied to an arbitrary potential $\phi(r)$, but for definiteness we here make a specific choice.

$$N_e = N_0 \exp \frac{e\phi(r)}{KT_e}. \qquad (2)$$

When Eq. (1) does not hold, more elaborate arguments, of the type which are here later presented with reference to the positive ions, can be employed to determine the electron distribution function.

Assume also that

$$-Ze\phi(R) \gg KT_i \gg -Ze\phi(\lambda). \qquad (3)$$

This suggests that in the region $r > \lambda$ collisional effects dominate the effects of the electrostatic field, and the distribution function is very closely Maxwell-Boltzmann, whereas in the region $R \leq r \leq \lambda$ collisions can be neglected and the ions move freely in the radial electric field.

Suppose that the distribution of ions with negative radial velocity, the potential, and the gradient of the potential are known at $r = \lambda$. In addition, assume that the properties of the probe as regards absorption, reflection, and re-emission of incident ions are known. Then the problem of determining the probe characteristic can be reduced to solving the Boltzmann equation

$$\frac{df}{dt} = \mathbf{v} \cdot \nabla f - \frac{Ze}{m} \nabla\phi \cdot \nabla_v f = 0 \qquad (4)$$

and Poisson's equation

$$\nabla^2\phi = -4\pi e(ZN_i - N_e) \qquad (5)$$

jointly in the region $R \leq r \leq \lambda$. The function $f(\mathbf{r}, \mathbf{v})$ is the joint distribution in position and velocity of the ions. Equation (4) states that in the absence of collisions f is constant along an ion trajectory, the time derivative d/dt being taken along said trajectory. The ion number density N_i and mean velocity $\mathbf{V}_i$ are given by

$$N_i = \int d^3\mathbf{v}\, f, \qquad (6)$$

$$N_i\mathbf{V}_i = \int d^3\mathbf{v}\, \mathbf{v}\, f. \qquad (7)$$

It is clear from Eq. (4) that the general solution of Eq. (4) is an arbitrary function of the constants of motion.[2] As is well known,[4] in a central field a particle orbit lies in a plane passing through the origin. Apart from orientation in that plane, it is characterized by two constants of the motion, the energy E, and the magnitude of the angular momentum J. Because of the spherical symmetry it follows that all planes of motion, and all orientations of orbit in a given plane are equivalent, whence the general solution of Eq. (4) is

$$f = f(E, J). \qquad (8)$$

Consider a point whose position relative to the center of the probe is $\mathbf{r}$. Let $\mathbf{r}$ be the axis of a cylindrical coordinate system w, α, u in velocity space, where u is the component of $\mathbf{v}$ along $\mathbf{r}$, w the magnitude of the component of $\mathbf{v}$ perpendicular to $\mathbf{r}$, and α the azimuthal angle. Then

$$E = \frac{m}{2}(u^2 + w^2) + Ze\phi(r), \qquad (9)$$

$$J = mrw, \qquad (10)$$

where m is the ion mass. The inverse relations are

$$u = \pm[2(E - Ze\phi)/m - J^2/m^2r^2]^{\frac{1}{2}}, \qquad (11)$$

$$w = J/mr. \qquad (12)$$

Clearly one must set $f(E, J) = f^+(E, J) + f^-(E, J)$, where f^+ corresponds to $u > 0$ and f^- to $u < 0$. In general, because the probe is not perfectly reflecting, f^+ is not necessarily equal to f^-, and in order to establish the connection between them it is necessary to analyze the ion orbits. That is, suppose one is given $f^-(E, J)$ at $r = \lambda$, and suppose the potential $\phi(r)$ is known. Choose values of E and J, which selects a trajectory; $f^-(E, J)$ determines the number of ions moving radially inward on that trajectory. If as one decreases r there is a turning point in the radial motion before one strikes the probe, then $f^+(E, J) = f^-(E, J) = \frac{1}{2} f(E, J)$ for all greater values of the radius, while $f(E, J) = 0$ for all lesser values. If, however, the orbit strikes the probe then the connection between $f^+(E, J)$ and $f^-(E, J)$ is determined by the properties of the probe as regards absorption, reflection, and re-emission. It seems physically reasonable, and is mathematically convenient, to treat the probe as completely absorbing. In this case, for all r between R and λ, $f^+(E, J) = 0$, $f^-(E, J) = f(E, J)$. In principle, of course, an arbitrary connection between f^+ and f^- at $r = R$ can be handled.

In the region $r > \lambda$, where collisions dominate, the problem is more difficult. There it is necessary to solve jointly the Boltzmann equation with appropriate collision integrals on the right-hand side, and Poisson's equation. This has not proved feasible. However, if λ is large so that only a small region Ω of the E, J phase space corresponds to orbits that strike the probe, it is reasonable to suppose that $f^-(E, J)$ is almost Maxwellian, being

[4] H. Goldstein, *Classical Mechanics* (Addison-Wesley Press, Cambridge, Massachusetts, 1950), Chap. 3, particularly p. 63 *et seq.*

only slightly decreased in and around the region Ω. Moreover, in the limit $\lambda \to \infty$ which is the convenient regime in which to work, one anticipates that $f^-(E, J)$ becomes strictly Maxwellian.

CLASSIFICATION OF ORBITS

The analysis of the orbits is most readily carried out in terms of the effective potential energy[4]

$$U(r, J) = Ze\phi(r) + J^2/2mr^2 \tag{13}$$

which governs the radial motion. The curves of U *versus* r at constant J^2 are shown schematically in Fig. 1. These have been drawn assuming that (a)

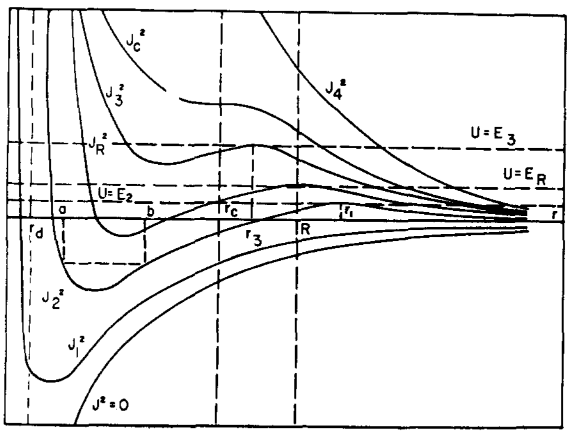

FIG. 1. Schematic diagram of the effective potential energy for the radial motion *versus* radius.

for small r, $r^2\phi(r)$ tends to zero as r decreases, and (b) for large r, the asymptotic behavior of the potential is

$$\phi(r) = \frac{\text{const}}{r^2} = -\frac{J_a^{\,2}}{2mr^2Ze}. \tag{14}$$

These assumptions will be justified *a posteriori*. The first of them implies that for small radius the centrifugal term $J^2/2mr^2$ dominates. The second determines the asymptotic behavior of $U(r, J)$.

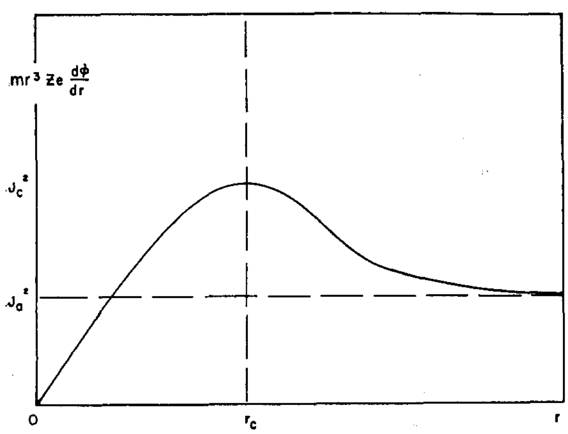

FIG. 2. Schematic plot of $mr^3Ze\ d\phi/dr$ *versus* radius.

The qualitative behavior of the curves can be seen readily. For large J^2 the centrifugal term everywhere dominates the electric potential, which latter increases monotonically to zero. The associated U curve thus decreases monotonically to zero. Now $(\partial U/\partial J^2)_r \geq 0$, whence as J^2 decreases the new curve lies below the old. The curves retain their monotonic decreasing character until J^2 has been reduced to a critical value $J_c^{\,2}$ where an inflection point is developed. For slightly smaller values of J^2 the curves exhibit a minimum followed by a maximum at some larger radius, after which they decrease monotonically to zero. When J^2 drops below $J_a^{\,2}$ [given by Eq. (14)], the behavior for larger r is dominated by $\phi(r)$ and the curves exhibit only a minimum, past which they increase monotonically to zero.

The location of the extrema is given by

$$\partial U/\partial r)_J = 0, \tag{15}$$

or

$$J^2 = mr^3Ze\ d\phi/dr. \tag{16}$$

A schematic plot of Eq. (16) is shown in Fig. 2. Clearly the angular momentum J_c is determined by the maximum of this curve, which occurs when

$$\frac{d}{dr}\left[r^3\frac{d\phi}{dr}\right] = 0. \tag{17}$$

Equation (17) serves to determine a critical radius r_c such that if the probe radius is less than r_c (for instance, equal to r_d as shown in Fig. 1), then there exist orbits which do not cut the probe, and which are of bounded radial variation. Such a one is indicated by the dashed horizontal line in the figure. It corresponds to a particle of angular momentum J_2, and energy $E = U(a, J_2) = U(b, J_2)$, where a and b are the turning points of the orbit. The population of ions on such trajectories is determined by collisions, however infrequent, and is most difficult to calculate. Thus, in order to obtain a tractable problem, let us consider only probe radii greater than r_c. This choice excludes the possibility of any such trapped ions, since all orbits to the left of a potential maximum (which may occur at $r = \infty$) intersect the completely absorbing probe, and are hence unpopulated.

Denote by $J_R^{\,2} = mR^3Ze\ d\phi(R)/dR$ the value of the square of the angular momentum associated with that effective potential energy curve which has its maximum at $r = R$. Ions of energy E for which $J^2 > J_R^2$ will be absorbed by the probe if $U(R, J) \leq E$, otherwise they will be reflected at some larger radius, since the maximum in the curve $U(r, J)$, if any, lies to the left of R. Ions of energy E for which $J^2 < J_R^2$ will be absorbed by the probe if E is greater than the value of U at the maximum of the associated effective potential energy curve. The locus in the E, J^2 phase space of these maxima is determined parametrically by Eqs. (13) and (16). Define in this phase space the curve $J^2 = G(E)$ via

$$\left.\begin{aligned} J^2 &= mr^3 Ze\, d\phi(r)/dr \\ E &= Ze\phi(r) + \tfrac{1}{2}Zer\, d\phi(r)/dr \end{aligned}\right\} J^2 \leq J_R^2 \quad (r \geq R), \tag{18}$$
$$J^2 = 2mR^2[E - Ze\phi(R)] \qquad J^2 \geq J_R^2.$$

Then, as depicted schematically in Fig. 3, region

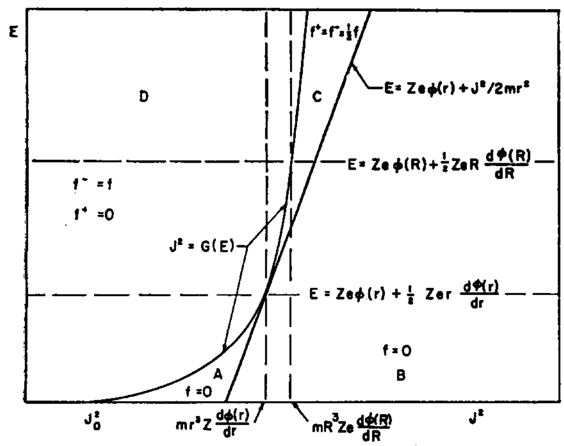

FIG. 3. Schematic diagram of the E, J^2 phase plane.

D to the left of this curve corresponds to orbits which strike the probe and thus in this region $f^+(E, J) = 0$, $f^-(E, J) = f(E, J)$.

Now at any radius the radial kinetic energy $\frac{1}{2}mu^2 = E - U(r, J)$ must be non-negative. Consider in the E, J^2 plane the straight line $E = U(r, J) = Ze\,\phi(r) + J^2/2mr^2$, for a given radius r. This line is tangent at one point to the curve $J^2 = G(E)$. Clearly the region B to the right of this line is excluded, and there $f = 0$.

The region A between the curves $J^2 = G(E)$ and $E = U(r, J)$ below the point of tangency is also excluded since it corresponds to orbits which intersect the probe and have a turning point to the left of the maximum in the associated effective potential energy curve. In the remaining region C, all orbits come in from $r = \infty$ and have a turning point at a radius greater than R. Thus in C, $f^+(E, J) = f^-(E, J) = \frac{1}{2}f(E, J)$.

EXPRESSIONS FOR THE DENSITY AND FLUX

Since the distribution function depends only on E and J it is convenient to employ these as the variables of integration in the integrals determining the ion current and density. To this end observe that one can write in terms of the coordinates w, α, u of the paragraph preceding Eq. (9)

$$d^3\mathbf{v} = dw\, w\, d\alpha\, du. \tag{19}$$

On introducing the set of variables J, α, E via Eqs. (9) and (10) one can write

$$d^3\mathbf{v} = d\alpha\, dE\, dJ J m^{-2} r^{-2} \{2m[E - Ze\phi(r)] - J^2/r^2\}^{-\frac{1}{2}}. \tag{20}$$

The density and drift velocity are then given by

$$N_i = \frac{2\pi}{m^2 r^2} \int_{C+D} \frac{dE\, dJ J\, f(E, J)}{\{2m[E - Ze\phi(r)] - J^2/r^2\}^{\frac{1}{2}}}, \tag{21}$$

$$N_i \mathbf{V}_i = -\mathbf{e}_r 2\pi \int_D dE\, dJ J\, f(E, J), \tag{22}$$

where the integration over α has been carried out.

Define

$$\begin{aligned} W(r) &= Ze\phi(r) + \tfrac{1}{2}Zer\, d\phi(r)/dr, \\ K(r, E) &= 2mr^2[E - Ze\phi(r)]. \end{aligned} \tag{23}$$

Then, on inserting the limits of integration in accordance with Fig. 3, Eqs. (21) and (22) can be written

$$\begin{aligned} N_i(r) &= (\pi/m^2r^2) \int_0^\infty dE \int_0^{G(E)} dJ^2\, f^-(E, J) \\ &\quad \cdot \{2m[E - Ze\phi(r)] - J^2/r^2\}^{-\frac{1}{2}} \\ &\quad + (\pi/m^2r^2) \int_{W(r)}^\infty dE \int_{G(E)}^{K(r,E)} dJ^2\, 2f^-(E, J) \\ &\quad \cdot \{2m[E - Ze\phi(r)] - J^2/r^2\}^{-\frac{1}{2}}, \end{aligned} \tag{24}$$

$$N_i(r)\mathbf{V}_i(r) = -\mathbf{e}_r(\pi/m^3r^2) \cdot \int_0^\infty dE \int_0^{G(E)} dJ^2 f^-(E, J). \tag{25}$$

Observe from Eq. (25) that the flux of ions at a given radius is proportional to r^{-2}, as it must be in order to conserve particles.

Equation (24) can now be inserted in Poisson's equation (4) which, on employing Eq. (2) for N_e and using a given $f^-(E, J)$, then represents a nonlinear integro-differential equation which determines $\phi(r)$.

If $\partial f^-/\partial J = 0$, as is the case for the Maxwell-Boltzmann distribution, $f^- = \frac{1}{2}(N_0/Z)e^{-E/KT_i}$, one can carry out the integration over J^2, obtaining

$$N_i = (2\pi/m^2) \int_0^\infty dE\, f^-(E)\{[2m(E - Ze\phi)]^{\frac{1}{2}} - [2m(E - Ze\phi) - G(E)/r^2]^{\frac{1}{2}}\} + (2\pi/m^2) \cdot \int_{W(r)}^\infty dE\, 2f^-(E)[2m(E - Ze\phi) - G(E)/r^2]^{\frac{1}{2}}, \tag{26}$$

$$N_i\mathbf{V}_i = -\mathbf{e}_r(\pi/m^3r^2) \int_0^\infty dE\, f^-(E)G(E). \tag{27}$$

Observe that even in the form of Eq. (26) the density is expressed in terms of the potential via an integral, in a very complicated fashion. Moreover it is not clear that f^-, as determined by collisions at $r = \lambda$ and beyond, is completely independent of J, since the probe acts as a sink for particles of small angular momentum.

Thus in order to get a tractable problem, in view of these uncertainties, it is reasonable to consider the case of monoenergetic ions, rather than the Maxwell distribution which at first glance might appear appropriate. One plausibility argument for this assumption is that the integration indicated in Eq. (26) tends to smooth out the differences between distribution functions.

MONOENERGETIC IONS

Choose

$$f^-(E) = \frac{m^2N_0}{4\pi Z} \frac{\delta(E - E_0)}{(2mE_0)^{\frac{1}{2}}}, \tag{28}$$

where $E_0 \sim KT_i$.

Poisson's equation (5) then reads, on employing Eqs. (2), (26), and (28),

$$\frac{1}{r^2}\frac{d}{dr}\left[r^2\frac{d\phi}{dr}\right] = -4\pi e^2N_0\left\{\frac{1}{2Z}\left[1 - \frac{Ze\phi(r)}{E_0}\right]^{\frac{1}{2}} - \frac{1}{2Z}\left[1 - \frac{Ze\phi(r)}{E_0} - \frac{G(E_0)}{2mE_0r^2}\right]^{\frac{1}{2}} + \frac{1}{Z}H[E_0 - W(r)]\left[1 - \frac{Ze\phi(r)}{E_0} - \frac{G(E_0)}{2mE_0r^2}\right]^{\frac{1}{2}} - e^{e\phi(r)/KT_e}\right\}, \tag{29}$$

where the step function $H(z)$ is unity if its argument is positive, and vanishes otherwise. The total ion flow to the probe is

$$I = -4\pi R^2\mathbf{e}_r\cdot N_i(R)\mathbf{V}_i(R) = \frac{\pi N_0G(E_0)}{m(2mE_0)^{\frac{1}{2}}}. \tag{30}$$

Observe that the condition that the argument of the step function vanish is, by Eq. (23),

$$E_0 = Ze\phi(r_0) + \tfrac{1}{2}Zer_0\, d\phi(r_0)/dr_0, \tag{31}$$

and by Eq. (18) corresponds to a potential energy curve characterized by

$$J_0^2 = G(E_0) = mr_0^3Ze\, d\phi(r_0)/dr_0, \tag{32}$$

which has its maximum at r_0. Thus when $E_0 - V(r_0)$ vanishes so does the argument of the square root which multiplies it. Hence if one introduces the dimensionless variables

$$\begin{aligned} \xi &= r[4\pi N_0e^2Z/KT_e]^{\frac{1}{2}}, \\ \iota &= 2I(Ze^2/KT_e)(2KT_e/m)^{-\frac{1}{2}}, \\ \beta &= E_0/ZKT_e, \\ \chi &= -e\phi/KT_e, \end{aligned} \tag{33}$$

Eq. (29) reads

$$\begin{aligned} \frac{1}{\xi^2}\frac{d}{d\xi}\left[\xi^2\frac{d\chi}{d\xi}\right] &= \tfrac{1}{2}\left[1 + \frac{\chi}{\beta}\right]^{\frac{1}{2}} + \tfrac{1}{2}\left[1 + \frac{\chi}{\beta} - \frac{\iota}{\beta^{\frac{1}{2}}\xi^2}\right]^{\frac{1}{2}} - e^{-\chi}, \quad \xi \geq \xi_0 \\ &= \tfrac{1}{2}\left[1 + \frac{\chi}{\beta}\right]^{\frac{1}{2}} - \tfrac{1}{2}\left[1 + \frac{\chi}{\beta} - \frac{\iota}{\beta^{\frac{1}{2}}\xi^2}\right]^{\frac{1}{2}} - e^{-\chi}, \quad \xi \leq \xi_0 \end{aligned} \tag{34}$$

where ξ_0 is determined by

$$\begin{aligned} 1 + \frac{\chi(\xi_0)}{\beta} - \frac{\iota}{\beta^{\frac{1}{2}}\xi_0^2} &= 0, \\ \frac{d}{d\xi_0}\left[1 + \frac{\chi(\xi_0)}{\beta} - \frac{\iota}{\beta^{\frac{1}{2}}\xi_0^2}\right] &= 0. \end{aligned} \tag{35}$$

Equation (34) is to be solved subject to the condition that

$$\lim_{\xi\to\infty} \chi = 0. \tag{36}$$

Note that in the limit of large ξ Eq. (34) can be solved approximately by equating to zero the right-hand side. This yields the so-called plasma solution which in this case reads

$$\frac{1}{\xi^2} = \frac{\beta^{\frac{1}{2}}}{\iota}\left\{1 + \frac{\chi}{\beta} - \left[2e^{-\chi} - \left(1 + \frac{\chi}{\beta}\right)^{\frac{1}{2}}\right]^2\right\}. \tag{37}$$

On appropriate expansion as $\chi \to 0$ ($\xi \to \infty$), Eq. (37) yields

$$\chi = \frac{\beta^{\frac{1}{2}}\iota}{2 + 4\beta}\frac{1}{\xi^2}, \tag{38}$$

which is the behavior assumed in the analysis of the orbits [see Eq. (14)]. This asymptotic behavior can be shown to follow in general by a straightforward if tedious asymptotic analysis of Poisson's equation in the general case.

Equation (34) has been integrated numerically on the IBM 704 at the U.S. Atomic Energy Commission Computing Center at New York University. The results are presented in Figs. 4 through 8.[5] The representative curves of Figs. 4 and 5 have been terminated at that radius where the possibility of trapped particles enters. Observe that, contrary to what has been believed,[3] there is an appreciable dependence on ion temperature, sufficient (see Fig. 8) to offer perhaps some hope of using measurements of positive ion current to estimate ion temperature, if the electron temperature is known.

The case $\beta = 0$, considered by Allen *et al.*,[1] is recovered from Eq. (34) in the limit $\beta \to 0$. In this limit $\xi_0 \to \infty$, while

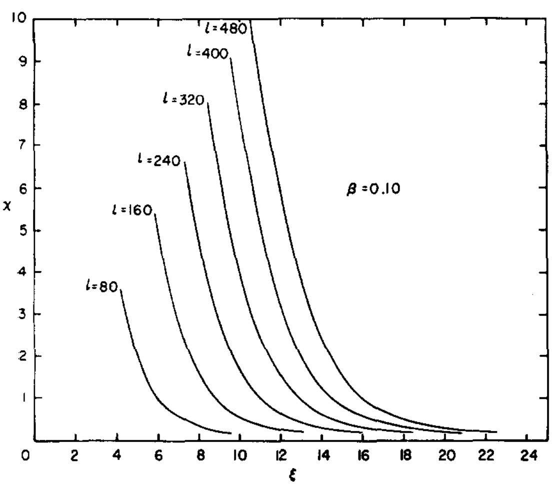

FIG. 4. Plot of probe potential *versus* radius for a spherical probe; $\iota = 80, 160, 240, 320, 400, 480$; $\beta = 0.10$.

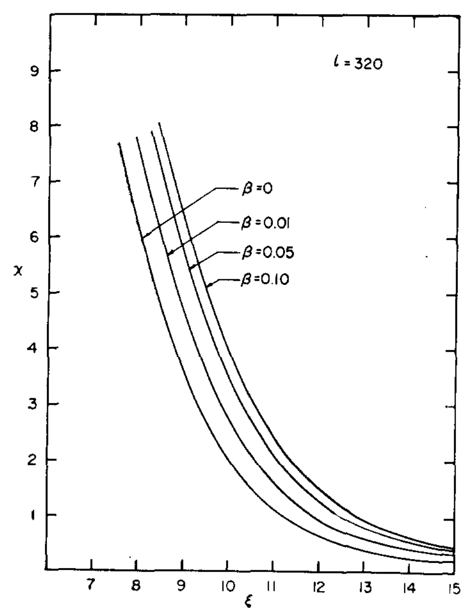

FIG. 5. Plot of potential *versus* radius for a spherical probe; $\iota = 320$; $\beta = 0, 0.01, 0.05, 0.10$.

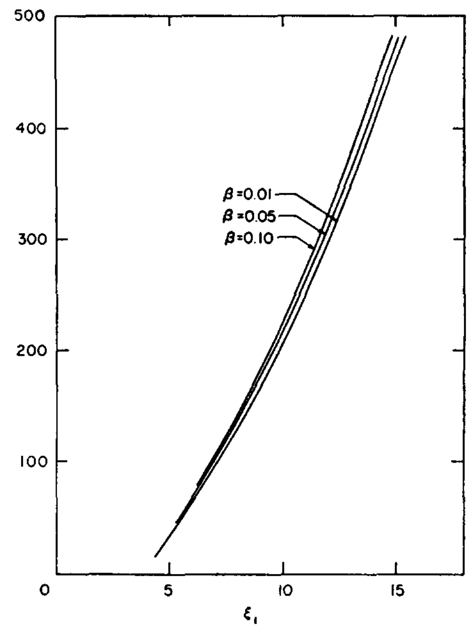

FIG. 6. Plot of the radius below which trapped ions are possible *versus* ion current for a spherical probe.

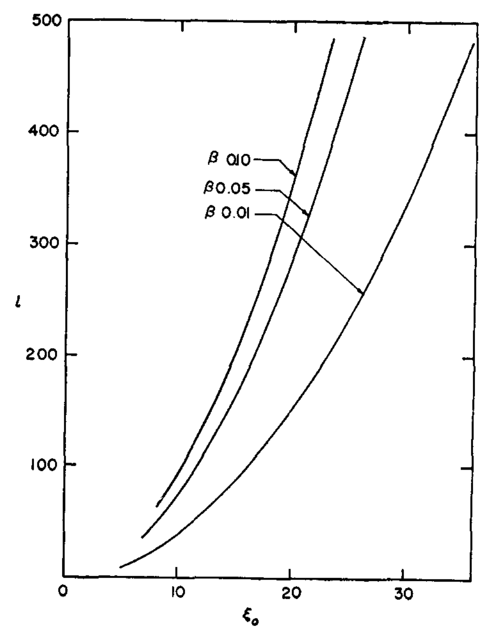

FIG. 7. Plot of the radius at which there is a maximum in a curve of effective potential at the energy E_0 under consideration, for a spherical probe.

[5] Numerical tables are available on request in the authors' unpublished report: Project Matterhorn, U. S. Atomic Energy Commission Research and Development Rept. PM-S-38 (October 17, 1958).

$$\frac{1}{\xi^2}\frac{d}{d\xi}\left[\xi^2\frac{d\chi}{d\xi}\right] = \lim_{\beta\to 0}\left\{\frac{1}{2}\left[1+\frac{\chi}{\beta}\right]^{\frac{1}{2}} - \frac{1}{2}\left[1+\frac{\chi}{\beta}-\frac{\iota}{\beta^{\frac{1}{2}}\xi^2}\right]^{\frac{1}{2}} - e^{-\chi}\right\}$$
$$= \lim_{\beta\to 0}\left\{\frac{1}{2}\frac{\iota/\beta^{\frac{1}{2}}\xi^2}{\left[1+\frac{\chi}{\beta}\right]^{\frac{1}{2}} + [1+(\chi/\beta)-(\iota/\beta^{\frac{1}{2}}\xi^2)]^{\frac{1}{2}}} - e^{-\chi}\right\} = \frac{\iota}{4\chi^{\frac{1}{2}}\xi^2} - e^{-\chi}, \tag{39}$$

which, apart from notation, is the equation they considered.

Consider Fig. 8. It is essentially the probe characteristic. Observe that only the region $\chi > 3$ is significant, since for smaller values the electron current would be appreciable. Note that the curves do not approach vertical lines as asymptotes, which would correspond to positive ion saturation. The reason for this is that as one increases χ the effective sheath radius increases also (see Fig. 4) and hence the total ion current incident on the sheath. In practice, however, the plasma is not infinite in extent, and cannot provide arbitrarily large ion currents to the probe. Hence measured probe characteristics may well show saturation.

CYLINDRICAL PROBE

The case of the infinite cylindrical probe can be handled in the same fashion as the spherical probe. Here it is convenient to employ the constants of the motion

$$\begin{aligned} E_\perp &= \tfrac{1}{2}m[\dot\rho^2 + \rho^2\dot\theta^2], \\ J &= m\rho^2\dot\theta, \\ E_\parallel &= \tfrac{1}{2}m\dot z^2, \end{aligned} \tag{40}$$

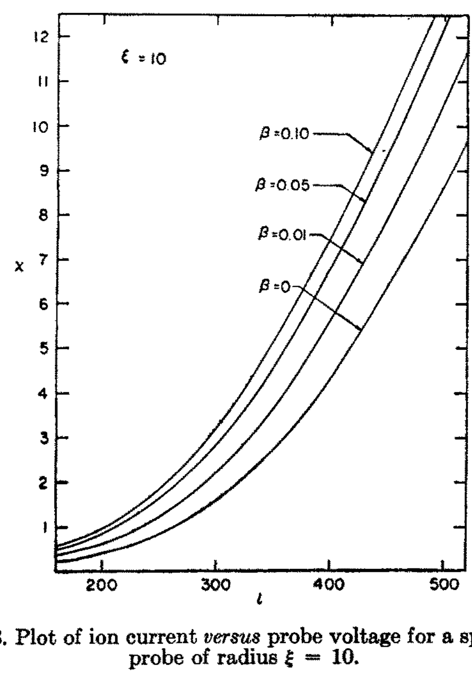

FIG. 8. Plot of ion current *versus* probe voltage for a spherical probe of radius $\xi = 10$.

and r, θ, z are the usual cylindrical coordinates in a system coaxial with the probe. Thus

$$\begin{aligned} \dot\rho &= \pm\{2[E_\perp - Ze\phi(\rho)]^{\frac{1}{2}} - J^2/m^2\rho^2\}^{\frac{1}{2}}, \\ \dot\theta &= J/m\rho^2, \\ \dot z &= \pm(2mE_\parallel)^{\frac{1}{2}}, \end{aligned} \tag{41}$$

and the distribution function $f(E_\perp, J, E_\parallel)$ must be decomposed into four parts according as the choice of signs of the square roots in Eqs. (41). The domain of $E_\parallel$ is $0 \le E_\parallel \le \infty$, independent of the values of J and $E_\perp$. The domain of integration of $E_\perp$ and J is determined from Fig. 3 where $E_\perp$ is to be identified with E, and ρ with r.

It is plausible to assume that the particle populations for given $\dot\rho$, $|\dot\theta|$, and $|\dot z|$ are independent of the sign of $\dot\theta$ and $\dot z$. If so, as will henceforth be assumed, one can write

$$\begin{aligned} N_i = {} & 2\int_0^\infty dE_\parallel \int_0^\infty dE_\perp \int_0^{G(E_\perp)^{\frac{1}{2}}} dJ \\ & \cdot f^-(E_\perp, J, E_\parallel)(2mE_\parallel)^{-\frac{1}{2}} \\ & \cdot m^{-1}\{2m\rho^2[E_\perp - Ze\phi(\rho)] - J^2\}^{-\frac{1}{2}} \\ & + 2\int_0^\infty dE_\parallel \int_{V(\rho)}^\infty dE_\perp \int_{G(E_\perp)^{\frac{1}{2}}}^{\{2m\rho^2[E_\perp - Ze\phi(\rho)]\}^{\frac{1}{2}}} dJ \\ & \cdot 2f^-(E_\perp, J, E_\parallel)(2mE_\parallel)^{-\frac{1}{2}} \\ & \cdot m^{-1}\{2m\rho^2[E_\perp - Ze\phi(\rho)] - J^2\}^{\frac{1}{2}}, \end{aligned} \tag{42}$$

$$\begin{aligned} N_i\mathbf{V}_i = {} & -\mathbf{e}_\rho 2\rho^{-1}m^{-2}\int_0^\infty dE_\parallel \int_0^\infty dE_\perp \\ & \cdot \int_0^{G(E_\perp)^{\frac{1}{2}}} dJ\; 2f^-(E_\perp, J, E_\parallel)(2mE_\parallel)^{-\frac{1}{2}}. \end{aligned} \tag{43}$$

Assume that f^- is independent of J. Then if one carries out the integration over J,

$$\begin{aligned} N_i = {} & 2\int_0^\infty dE_\parallel(2mE_\parallel)^{-\frac{1}{2}} \int_0^\infty dE_\perp f^-(E_\perp, E_\parallel) \\ & \cdot m^{-1} \arcsin\left\{\frac{G(E_\perp)}{2m\rho^2[E_\perp - Ze\phi(\rho)]}\right\}^{\frac{1}{2}} \\ & + 4\int_0^\infty dE_\parallel(2mE_\parallel)^{-\frac{1}{2}} \int_{V(\rho)}^\infty dE\, f^-(E_\perp, E_\parallel) \\ & \cdot m^{-1}\left[\frac{\pi}{2} - \arcsin\left\{\frac{G(E_\perp)}{2m\rho^2[E_\perp - Ze\phi(\rho)]}\right\}^{\frac{1}{2}}\right], \end{aligned} \tag{44}$$

$$N_i\mathbf{V}_i = -\mathbf{e}_\rho 2m^{-2}\rho^{-1}\int_0^\infty dE\,(2mE_\parallel)^{-\frac{1}{2}} \cdot \int_0^\infty dE_\perp\, f^-(E_\perp, E_\parallel)G(E_\perp)^{\frac{1}{2}}. \tag{45}$$

For simplicity choose

$$f^-(E_\perp, J, E_\parallel) = \frac{N_0}{Z}\frac{m}{2\pi}\,\delta(E_\perp - E_0) \cdot \frac{g(E_\parallel)}{\int_0^\infty dE_\parallel\, g(E_\parallel)(2mE_\parallel)^{-\frac{1}{2}}}. \tag{46}$$

Then

$$N_i = \frac{N_0}{\pi Z}\arcsin\left\{\frac{G(E_0)}{2m\rho^2[E_0 - Ze\phi(\rho)]}\right\}^{\frac{1}{2}} + \frac{2N_0}{\pi Z}H[E_0 - V(\rho)] \cdot\left[\frac{\pi}{2} - \arcsin\left\{\frac{G(E_0)}{2m\rho^2[E_0 - Ze\phi(\rho)]}\right\}^{\frac{1}{2}}\right], \tag{47}$$

$$N_i\mathbf{V}_i = -\mathbf{e}_\rho\,\frac{N_0G(E_0)^{\frac{1}{2}}}{m\rho Z}. \tag{48}$$

Note that the total particle current per unit length to the probe is

$$I = 2\pi N_0G(E_0)^{\frac{1}{2}}/mZ. \tag{49}$$

Introduce the dimensionless quantities

$$\begin{aligned} \chi &= -e\phi/KT_e, \\ \xi &= \rho[4\pi Ze^2N_0/KT_e]^{\frac{1}{2}}, \\ \iota &= (1/\pi)(Ze^2/KT_e)(m/2E_0)(I^2/N_0), \\ \beta &= E_0/ZKT_e. \end{aligned} \tag{50}$$

Then Poisson's equation (5) reads, on employing Eqs. (2), (47), and (50),

$$\begin{aligned} \frac{1}{\xi}\frac{d}{d\xi}\left[\xi\frac{d\chi}{d\xi}\right] &= 1 - \frac{1}{\pi}\arcsin\left[\frac{\iota/\xi^2}{1+\chi/\beta}\right]^{\frac{1}{2}}, & \xi \ge \xi_0, \\ &= \frac{1}{\pi}\arcsin\left[\frac{\iota/\xi^2}{1+\chi/\beta}\right]^{\frac{1}{2}}, & \xi \le \xi_0, \end{aligned} \tag{51}$$

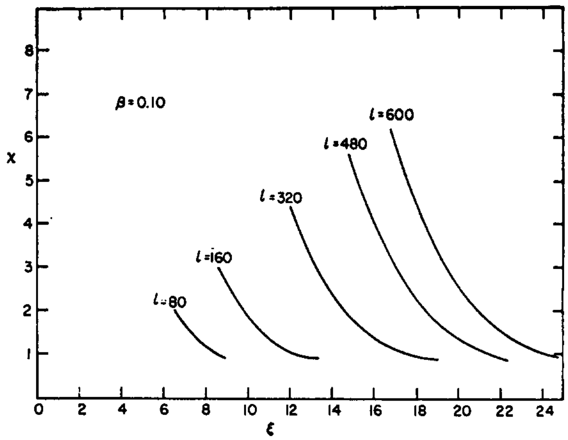

FIG. 9. Plot of probe potential *versus* radius for a cylindrical probe; ι = 80, 160, 240, 320, 400, 480; β = 0.10.

where

$$\begin{aligned} \beta + \chi(\xi_0) - \beta\iota/\xi_0^2 &= 0, \\ (d/d\xi_0)[\beta + \chi(\xi_0) - \beta\iota/\xi_0^2] &= 0. \end{aligned} \tag{52}$$

Here the asymptotic behavior is ϕ = const/r as can be shown in general.

The results of the numerical solution of Eq. (51) are presented in Figs. 9, 10, 11, and 12.[5]

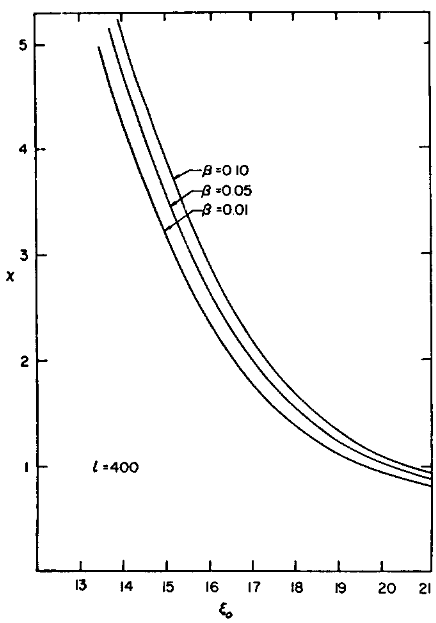

FIG. 10. Plot of potential *versus* radius for a cylindrical probe; ι = 400; β = 0.01, 0.05, 0.10.

ACKNOWLEDGMENT

The authors wish to acknowledge their indebtedness to their colleagues at Project Matterhorn for

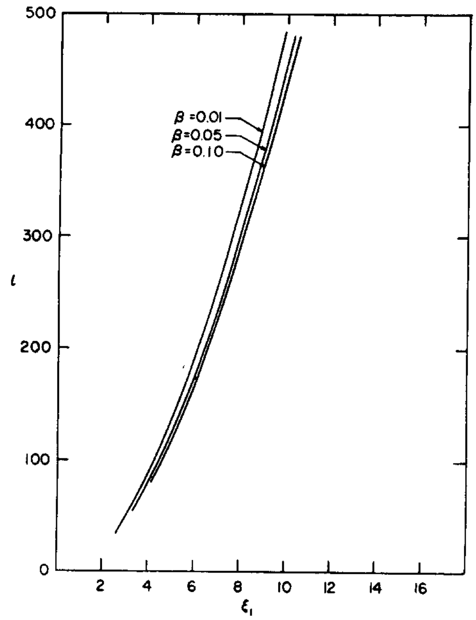

FIG. 11. Plot of the radius below which trapped ions are possible *versus* ion current, for a cylindrical probe.

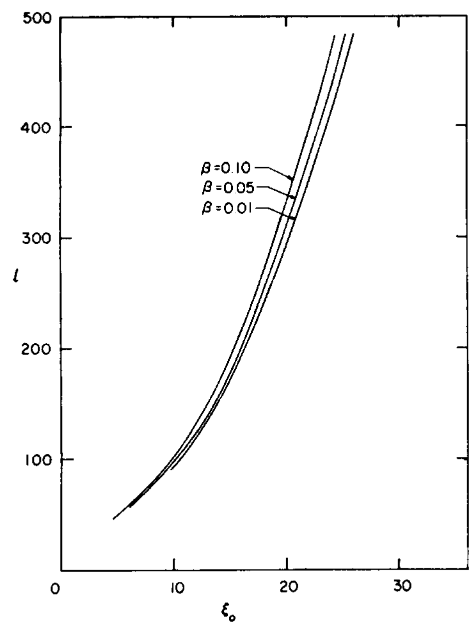

FIG. 12. Plot of the radius at which there is a maximum in the curve of effective potential energy at the energy E_0 in question, for a cylindrical probe.

their stimulating criticism, to Joan Peskin and Harold Vandenburgh for assistance in the numerical work, and to Francis F. Chen and Professor Lyman Spitzer for their critical reading of the manuscript.

APPENDIX

Note on Numerical Procedure

For computational purposes it was convenient to employ in Eq. (34) the variables

$$x = \iota^{\frac{1}{2}}\beta^{-\frac{1}{4}}\xi^{-1}, \qquad y = \chi\beta^{-1}. \tag{A-1}$$

This leads to the differential equation

$$\begin{aligned}\lambda x^4 \frac{d^2y}{dx^2} &= \tfrac{1}{2}(1+y)^{\frac{1}{2}} + \tfrac{1}{2}(1+y-x^2)^{\frac{1}{2}} - e^{-\beta y}, \qquad x \leq x_0,\\ &= \tfrac{1}{2}(1+y)^{\frac{1}{2}} - \tfrac{1}{2}(1+y-x^2)^{\frac{1}{2}} - e^{-\beta y}, \qquad x \geq x_0.\end{aligned} \tag{A-2}$$

The parameter λ is given by

$$\lambda = \iota^{-1}\beta^{5/4}. \tag{A-3}$$

The quantity x_0, following Eqs. (35), is determined from

$$1 + y(x_0) - x_0^2 = 0, \qquad (d/dx_0)[1 + y(x_0) - x_0^2] = 0. \tag{A-4}$$

Moreover

$$y(0) = 0. \tag{A-5}$$

Now for $x \sim 0$ one can obtain an asymptotic solution to Eq. (A-2) by setting the right-hand side of Eq. (A-2) equal to zero, which can be improved by iteration. This asymptotic solution, however, differs from the true solution by a one-parameter family of subdominant terms exponentially small in $1/x$. Thus it is not feasible to start the numerical integration at $x = 0$ since the determination of the subdominant terms is extremely difficult, and they make the numerical integration highly sensitive.

The equation was therefore solved by choosing a value of x_0 which determines $y(x_0)$ and $dy(x_0)/dx_0$ via Eqs. (A-4). The problem then reduced to choosing the parameter λ so that on inward integration the solution passed through the origin. Because of the sensitivity of the differential equation, it was never possible actually to carry the numerical solution through the origin, but nevertheless the "eigenvalue" λ could be determined to eight significant figures. Once λ was so found, the outward integration could be pursued in a straightforward manner.

The case $\beta = 0$ was degenerate, for there $x_0 \to 0$.

However, the subdominant terms vanished and the numerical integration was started by developing an asymptotic series for y in powers of x^2 and carrying it to x^{22}.

Equation (51) for the cylindrical probe was handled in analogous fashion. These calculations strongly suggest that all such self-consistent calculations in plasmas where shielding is important will lead to similar asymptotic problems, where great care is required for their numerical solution.

THE PHYSICS OF FLUIDS VOLUME 2, NUMBER 2 MARCH-APRIL, 1959

Some Exact Solutions of the Navier-Stokes and the Hydromagnetic Equations*

WILLIAM C. MEECHAM
Department of Physics, The University of Michigan, Ann Arbor, Michigan
(Received September 15, 1958)

Some exact, closed-form solutions of the Navier-Stokes equations for incompressible flow and of the hydromagnetic equations for high-conductivity, incompressible flow are presented. They can be considered to be generalizations of Taylor's solutions. The solutions are two dimensional and cellular containing a single-space Fourier component; the spatial behavior is chosen in such a way that the nonlinear inertial term and the pressure term cancel one another, leaving a linear system to be solved. The time behavior of the solutions is quite general. The solutions to the hydromagnetic equations are such that the velocity and the magnetic fields are parallel and decoupled. The velocity behaves as it does in the purely mechanical case while the magnetic field simply decays in time; there is no source term for it in the present treatment.

I. INTRODUCTION

A FEW exact, closed-form solutions to the Navier-Stokes equations for incompressible fluid flow are known. These solutions can in the main be classified as of Poiseuille type, involving fluid flow between parallel planes or down cylinders, and Couette type, involving circular flow between concentric cylinders. The known exact solutions to the full hydromagnetic equations are straightforward generalizations of the hydrodynamical solutions. It is the purpose of this paper to present a class of solutions to the Navier-Stokes and to the hydromagnetic equations. They are essentially generalizations of some of Taylor's exact solutions.[1] The solutions are two dimensional and cellular and yield velocity and magnetic fields described by a single Fourier space component. The Navier-Stokes equation is solved when the forcing term consists of a single Fourier space component plus an arbitrary vector function of time. The resulting velocity field consists of a space-constant average flow (corresponding to the space-constant force field) plus the single Fourier space component flow which has already been mentioned. With a magnetic field present, a solution of the initial value magnetic problem is obtained when the mechanical forcing term is simplified. The magnetic field is parallel to the velocity field and thus has the same cellular structure. When there is no magnetic field, the velocity field decays exponentially when the "cellular" force is turned off; the decay is due to the viscous loss term. When the magnetic field is present, the fields decay exponentially in time, at different rates, due to the effects of viscosity and Joulian heating.

The cellular character will be seen to be reminiscent of the von Kármán vortex street, although the present solutions differ in that they form a vortex lattice, are rotational in general, and take into account the effect of viscosity. In addition to Taylor's earlier work Taylor and Green[1] have considered periodic, or cellular, solutions of the incompressible, hydrodynamic equations in three dimensions. They examined the breakup of initial large eddies into smaller eddies as time progresses. In the present treatment, as already mentioned, there are no such effects.

II. BASIC EQUATIONS OF INCOMPRESSIBLE MAGNETOHYDRODYNAMICS

The theory of incompressible magnetohydrodynamics in a medium of high electrical conductivity

* This work was supported in part by Project MICHIGAN under a contract between the U. S. Army Signal Corps and The University of Michigan Research Institute.

[1] G. I. Taylor, Phil. Mag. **46**, 671 (1923); G. I. Taylor and A. E. Green, Proc. Roy. Soc. (London) **A158**, 499 (1937).